

# THERMOHYDRAULIC ANALYSIS OF A FUEL ELEMENT OF THE AP1000 REACTOR WITH THE USE OF MIXED OXIDES OF U / Th USING THE COMPUTATIONAL FLUID DYNAMIC CODE (CFX)

Caio J. C. M. R. Cunha<sup>1,2</sup>, Daniel G. Rodríguez<sup>2</sup>, Carlos A. B. O. Lira<sup>1,2</sup>, Giovanni L. Stefani<sup>3</sup> and Fernando R. A. Lima<sup>1,2</sup>

<sup>1</sup> Departamento de Energia Nuclear - UFPE  
Av. Professor Luís Freire 1000  
50740-545 Recife, PE, Brazil  
[caimiranda.engquimico@outlook.com](mailto:caimiranda.engquimico@outlook.com)

<sup>2</sup> Centro Regional de Ciências Nucleares do Nordeste (CRNC-NE / CNEN)  
Av. Professor Luís Freire 200  
50730-120 Recife, PE, Brazil  
[danielgonro@gmail.com](mailto:danielgonro@gmail.com); [cabol@ufpe.br](mailto:cabol@ufpe.br); [falima@cnen.gov.br](mailto:falima@cnen.gov.br)

<sup>3</sup> Instituto de Pesquisas Energéticas e Nucleares (IPEN / CNEN - SP)  
Av. Professor Lineu Prestes 2242  
05508-000 São Paulo, SP, Brazil  
[laranjogiovanni@gmail.com](mailto:laranjogiovanni@gmail.com)

## ABSTRACT

The present work carried out a thermohydraulic analysis of a typical fuel assembly of the reactor AP1000 changing the type of fuel, of  $UO_2$  conventionally used for a mixture of oxides of (U,Th) $O_2$  realizing some simplifications in the original design, with the objective to develop of an initial methodology capable of predicting the thermohydraulic behavior of the reactor within the limits established by the manufacturer. An expression for the power density was determined using a coupled neutronic-thermohydraulic calculation; once the final expression for power density was determined, the axial and radial temperature profiles in the assembly, as well as the pressure drop and the distribution of the coolant density, were evaluated. Due to the increase in research done on thorium, such as the work of [1], [2], [3], [4] and [5], as well as the mass diffusion of the AP1000, as is the case with [6] and [7]. The present study developed a simplified model, where burnable poisons and spacer grids were not considered, however, it is a consistent model, but with the insertion of these, a more accurate representation of the reactor is expected, providing operational transient analyzes. This tends to strengthen the lines of research that have been carrying out work on the AP1000, as well as in the general sphere of nuclear power plants.

## 1. INTRODUCTION

Thorium is a metallic element of the actinide class and is found in great abundance in the Earth's crust, so that it has on average three times more than the amount of available uranium, reaching 6000 parts per billion (ppb). This element is commonly found as the isotope  $Th^{232}$  (100%) with a half-life of  $1,4 \times 10^{10}$  years and having the production of several isotopes from its natural decay process until it becomes stable in  $Pb^{208}$  [8].

The forms in which thorium is normally found are: oxides, phosphates, and silicates. One of the interesting characteristics of this element is its high melting point, whose value is 3300°C being much larger than the 2800°C of the sintered UO<sub>2</sub>. Another important point is the decrease in the release of gases from fissions [9]. Thorium dioxide (ThO<sub>2</sub>) is relatively inert and does not oxidize more, the opposite of UO<sub>2</sub>, in addition to having high thermal conductivity and low coefficient of expansion compared to UO<sub>2</sub>. According to these properties, the use of thorium in the form of mixed oxides leads to an improvement in the thermoforming patterns, making it attractive in terms of application of a nuclear power plant fuel [10].

The availability of resources related to thorium on the earth's surface is vast, so it tends to be larger than those of uranium and fossil fuels combined. However, there is no way to classify thorium related sources; therefore, estimates of the quantity of these resources are made with respect to uranium and also so-called rare-earth.

Since the beginning of the development of nuclear energy, thorium has been considered as a potential fuel, mainly due to its ability to produce the fissile isotope U<sup>233</sup> [11]. Thorium fuel cycles may offer, besides those presented, certain advantages over the current fuel cycles in commercial use, since they produce much less plutonium and actinides than those based on U<sup>235</sup> and Pu<sup>239</sup>, where the plutonium can still be combined with thorium to achieve even greater elimination of itself.

In the context of generation III+ reactors, the most technologically recognized class is the pressurized water reactors (PWR), where among them, it is one of the most outstanding in terms of safety and reliability, which is the AP1000 [12]. Another factor of interest is the economic question regarding the useful life of the PWR reactors, which is situated in a range between 40 and 60 years [13], making them advantageous to develop a better utilization of resources available.

## 2. METHODOLOGY

### 2.1. Power Density Distribution in the Typical Fuel Assembly of AP1000 Reactor.

Initially, the axial distribution of energy released in the fuel elements with the code MCNP6 is calculated, considering a linear variation of the refrigerant temperature in a range of 288°C to 325°C, thus obtaining the initial values of the water density along with the height of the fuel assembly. From this calculation, the first axial density distribution of power which is inserted in the CFX, is obtained so as to obtain a new axial temperature distribution of the refrigerant and, consequently, a new axial distribution of the density of the water, which is again placed in the MCNP6 until the variation of the released energy reaches an established error and thereby obtains the definitive axial density distribution for the use in the CFX.

The power output along the height of the fuel assembly is made by dividing the total thermal power of the reactor (3400MW<sub>t</sub>) between the number of fuel assemblies (157), the number of fuel rods (264) and the volume of each cell over of the height, which is the volume of the fuel

divided by the number of cells (11 cells, for this case). Then this value is multiplied by a normalized power coefficient obtained in the calculation in each cell per height in MCNP6.

The neutronic modeling of the AP1000 reactor was performed in a simplified way, so that for the present study the structural data of the reactor was considered, however, wasn't considered any burnable poison presence. In order to establish a reliable model for further improvement, the air was considered in the control rod locations, as can see in Figure 1.

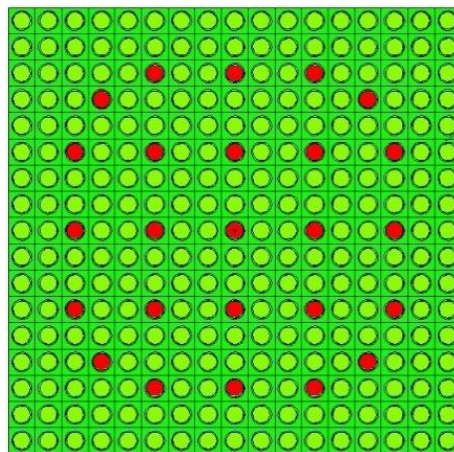


**Figure 1: Description of the fuel assembly used to the neutronic e thermohydraulic calculations.**

The Figure 1 illustrates the shape of the fuel assembly of the AP1000 reactor with the green circles representing fuel rods, red circles the control rod (which are considered air instead of burnable poisons) and the others spaces coolant fluids.

## **2.2. Description of the Computational Model Used for the Thermohydraulic Calculation of a Typical Fuel Assembly of the AP1000 reactor.**

### **2.2.1. Definition of the Reactor Geometry.**

The core of the AP1000 reactor, like the most common nuclear reactors, is composed of several rods (cylinders), be they fuel, control or instrumentation. When we delimit an area and form a structured group of bars, which varies with the type of reactor, we call by fuel assembly, in which, depending on the type of reactor varies the quantity and the format of these assemblies. In case of AP1000 they consist of a matrix 17x17 cylinders oriented vertically, totaling 289 cylinders, 24 of these tubes are guides for the insertion of control rods or burnable poisons, in addition to an instrumentation tube. The fuel elements have an active length of 426.72cm.

To perform the thermohydraulic study of the fuel assembly, it is necessary to construct the geometry of the same. For the present work, this geometry was developed from the *Design*

*Modeler* tool of Ansys software. To this end, the structural information provided in the reports released by Westinghouse (reactor builder) was used.

In order to simplify the calculations and optimize the computational resources available, due to the symmetry characteristics of the geometry it was possible to reduce to 1/8 of the complete fuel assembly. The design dimensions were maintained; however, it was only 28 complete cylinders, 16 cylinders halves and a cylinder with 1/8 of its radial length, forming a total of 45 elements, of which 39 corresponded to fuel rods and 6 control bars, according to Figure 2.

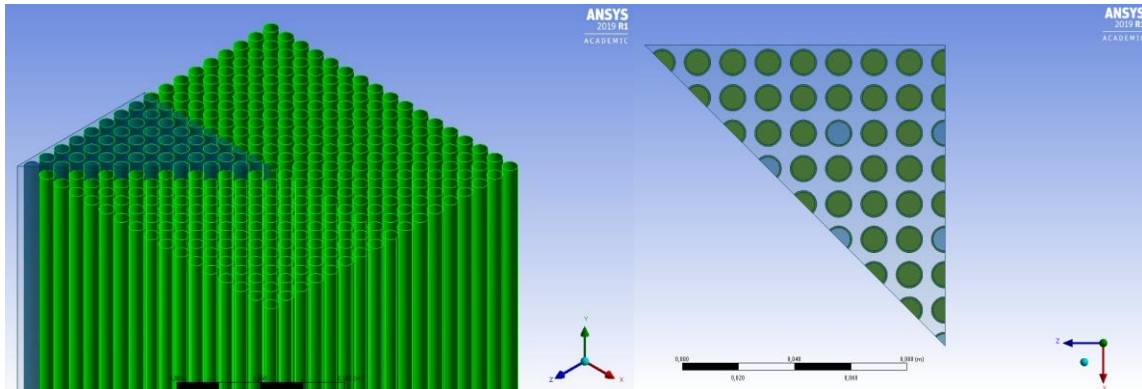


**Figure 2: Isometric and Superior View of the Geometry of the Fuel Assembly.**

The Figure 2 shows the simplifications performed in the present study such as: no insertion of spacer grids, no presence of burnable poisons, and reduction of geometry due to symmetry.

### **2.2.2. Calculation Method.**

The CFX code uses the finite volume method for the discretization of a domain using a mesh, so that variable values for the mass momentum and energy quantities are stored in these control volumes, constructed with the help of the mesh. When it comes to using of the finite volume method, the code uses “the vertex-centered” method, so that the control volume is formed by the combination of smaller sub-control volumes around the vertex, where the values of the variables are stored.

The shape of the mesh and the number of elements used to discretize the domain depend on the geometry and required precision of the solution. For the present work, the construction of the mesh was done through the Multizone method, which is based on the interweaving of independent zones, providing an automatic decomposition of the geometry in sweepable regions and free regions. When the Multizone method is selected, all regions interlace to form a pure hexahedral mesh, if possible. Aiming for a better adjustment of the mesh to the geometry, it was determined that the shape of the elements reach the projected structure, be of prism. This option is useful when the sources face can not be set and therefore the scanning method can no be applied. The mesh used in the discretization of the domain of the present work is presented in Figure 3.

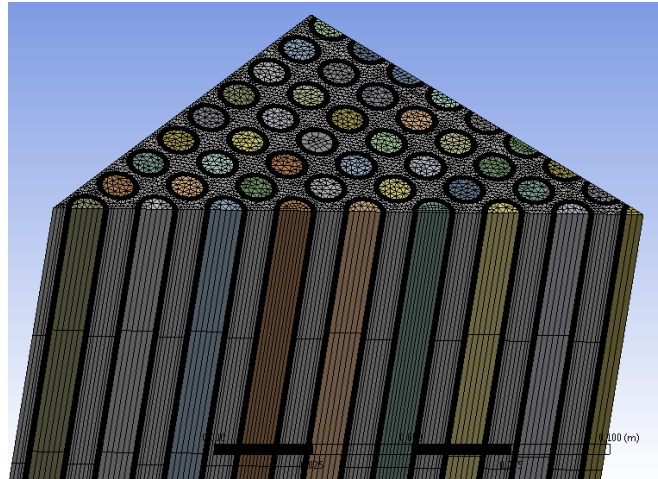


**Figure 3: Isometric View of the Mesh Used for Domain Discretization.**

In the present study, a structured mesh is used to adapt to the channel geometry. In the proximity of the walls, the mesh is refined to ensure that the velocity and temperature gradients are correctly solved, in addition to meeting all the requirements of the special treatment turbulence model close to the walls, which plays a significant role in the shear forces and the heat transfer coefficient. The mesh allowed for the current study object has 2399646 elements and 2636441 nodes; a number of internal divisions of 3 were applied to the gap and 5 to the cladding and coolant, in addition to having an average value of  $y^+$  of 32.43.

The mesh applied in the study was evaluated in 3 main parameters of quality, Asymmetry; Jacobian Ratio and Orthogonal Quality. Asymmetry which determines how close to ideal a face or cell is, that is, equilateral or equiangular, with 0 as ideal (great) and 1 for completely degenerated (worse), for the present work an average value of 0.1 was obtained, and can be considered optimal, in addition to 0.00092283 and 0.766325 as minimum and maximum values, respectively. For the Jacobian Ratio, which measures the shape of a given element and which influences the quality of the spatial mapping, so that the evaluation is done considering 1 for a great value and 0 for a bad, in the study we obtained 0.98372 as mean value, 0.25993 for the minimum and 1 for the maximum, characterizing a good result. The last and main parameter evaluated was the Orthogonal Quality, which, like the Jacobian Ratio, also considers 1 an optimal value and 0 a bad value, resulting in an average value of 0.94886, in addition to 0.23675 and 0.99962 for the minimum and maximum, respectively. In general, the mesh used showed good quality, favoring the reliability of the results.

### **2.2.3. Boundary Conditions.**

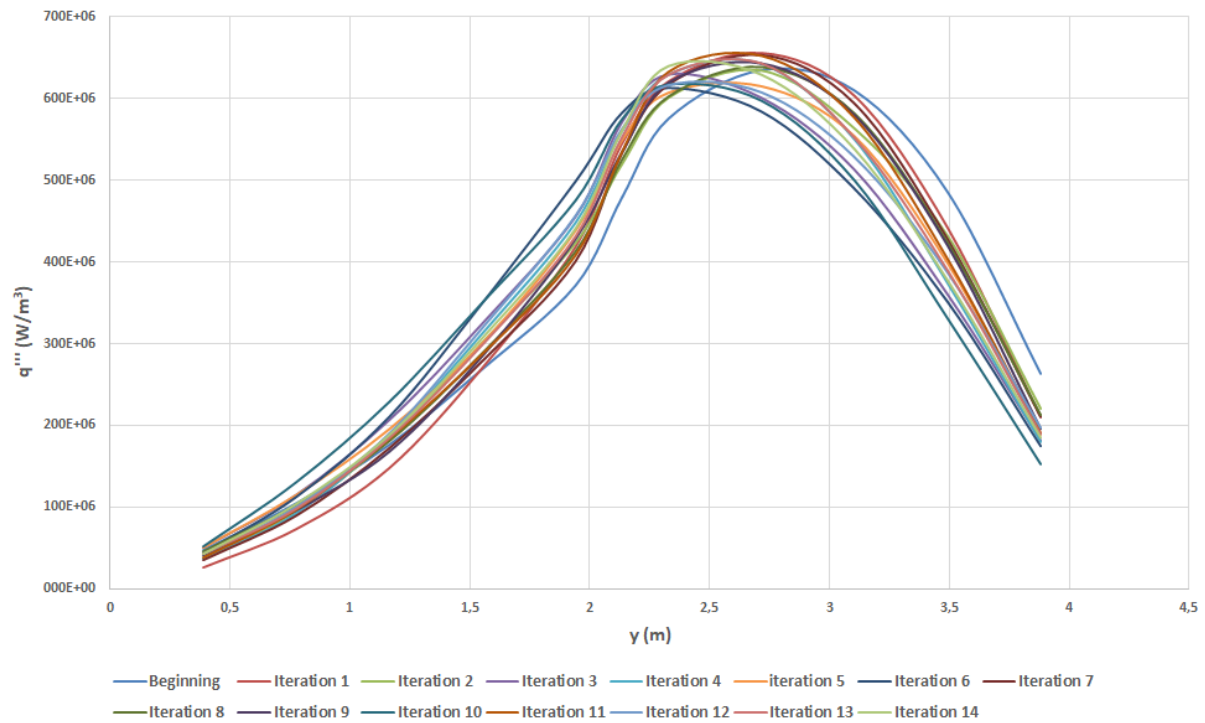
The inlet temperature of the refrigerant is admitted equal to the inlet in the core, is an approximation since said temperature should increase a few degrees from the inlet nozzle for the channels between the fuel elements. The properties of water were taken according to the International Association for Water Properties. From the library of materials provided by the software, IAPWS-IF97 was chosen, which is a formulation of water and steam properties prepared for industrial uses where formulations should be designed for fast and complex

calculations. These water properties are taken for the Steam51 Material which is a type of liquid water that is in this library for a temperature range ranging from 450 to 900K, which corresponds to a pressure range of 1MPa to 30MPa. Finally, the mass flow of refrigerant through 1/8 of the typical fuel assembly was determined by dividing the total mass flow entering the reactor core by the total number of fuel assemblies and also divided by 8.

### 3. RESULTS

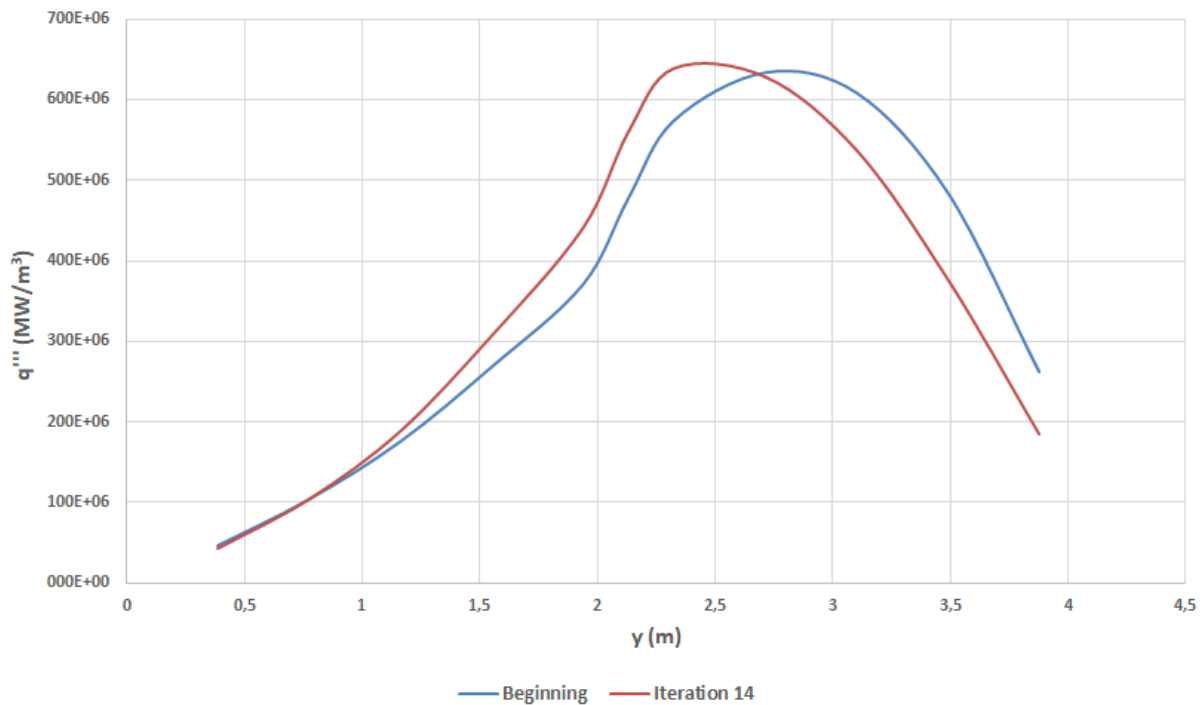
#### 3.1. Neutronic-Thermohydraulic Coupling.

With the need to obtain an expression that represents the parameter of connection between physics and reactor engineering, which is the power density, a neutronic-thermohydraulic couple calculation was used to insert this expression as an input data on CFX software. The iterative process is presented in Figure 4.



**Figure 4: Iterative Study of the Axial Distribution of Power Density.**

From Figure 4 it is observed that after 14 iteration as the final expression is obtained for the power density, that is, that the density of refrigerant has reached the stipulated error, which for the present case was 1%. Thus, a comparison was made between the initial and final states of the iterative process, as shown in Figure 5.



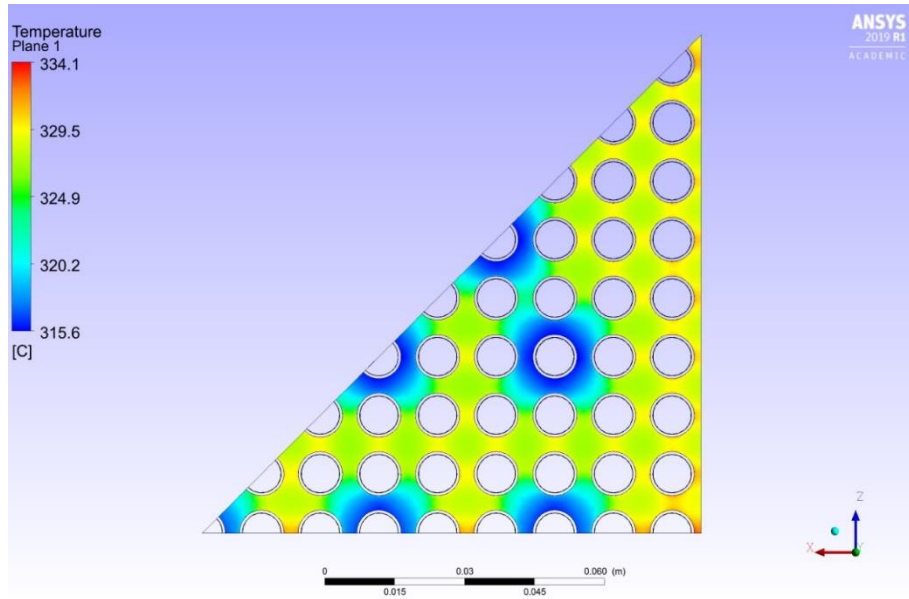
**Figure 5: Comparison of the Axial Distribution from the Power Density at Initial and Final States of the Iterative Process.**

Figure 4 illustrates the tendency that the region of higher heat generation has to approach the center of the fuel rod, being slightly higher for this type of reactor in question, since the coolant rises in the nucleus of the reactor. This approach to the end of the iterative process is evident in Figure 5.

### 3.2. Thermohydraulic Analysis.

After determining the expression of the axial distribution of power density, we proceeded to study the reactor AP1000, now in the scope of thermohydraulic, using only the CFX code for this. It is important to emphasize that the present study is aimed at the beginning of the cycle (BOC), that is, with fresh fuel, besides the non-application of burnable poisons. As a first result, it was possible to observe the temperature field at the exit of the fuel assembly, as shown in Figure 6. This, in turn, varies from 315,6°C, for regions near the guide tubes of the control rods, up to 334,1°C for the areas adjacent to the fuel rods.





**Figure 6: Coolant Temperature Field at the Fuel Assembly Outlet.**

According to the above figure the existence of low temperature zones is observed, the regions near the guides tubes of the control bars have lower temperatures those that surround the fuel rods since there is no generation of energy in these. Still in Figure 6, the average temperature was calculated on this exit plane and value just above 325°C was obtained, which is a good result since 325°C is the value reported in the manuals by Westinghouse. Another evaluation was made regarding the distribution of the refrigerant density and pressure along the fuel assembly, as shown in Figure 7.

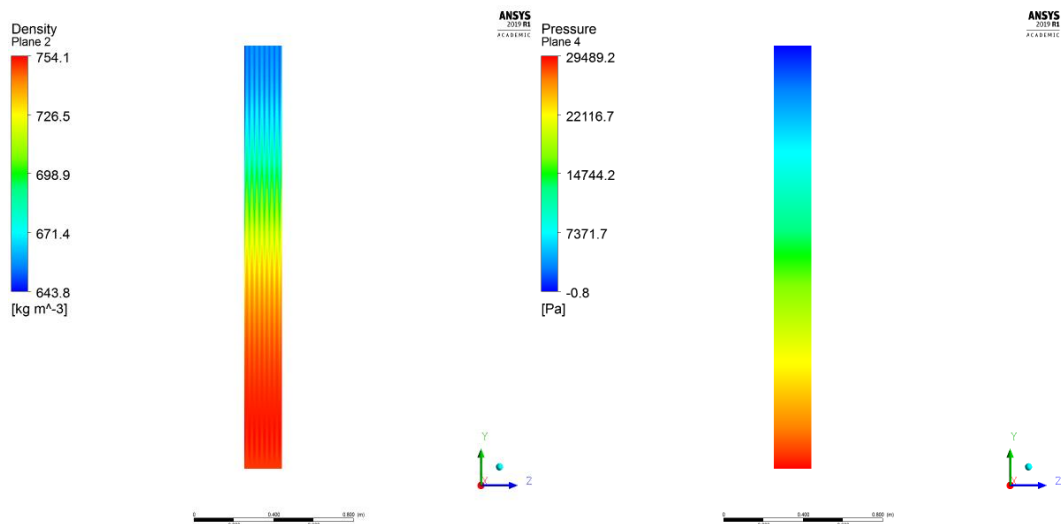


**Figure 7: Axial Distribution of Coolant Density and the Pressure Drop Along the Fuel Assembly.**



The variation in the temperature of the refrigerant, which is derived from the withdrawal of the heat generated by the fuel rods, in turn, causes in a variation of the density of the refrigerant fluid itself. For the present case, there was a variation of the order of 100kg for the density, which brought about a change in the pressure of 30kPa. This value obtained for the pressure drop is considered negligible if compared to the total pressure of the system, however, it should be noted that in the simulation were not considered spacer grids. These results are similar to those obtained by (Martínez, 2018), who simulated the AP1000 with a model similar to that employed in this work and obtained satisfactory results.

In order to evaluate the integrity of the fuel and other components of the bar, the axial and radial profiles of the temperature in the fuel rod were determined. First, the axial distribution of the temperature in the fuel centerline was obtained, in order to quantify and locate the point of greatest temperature in bar, as shown in Figure 8.

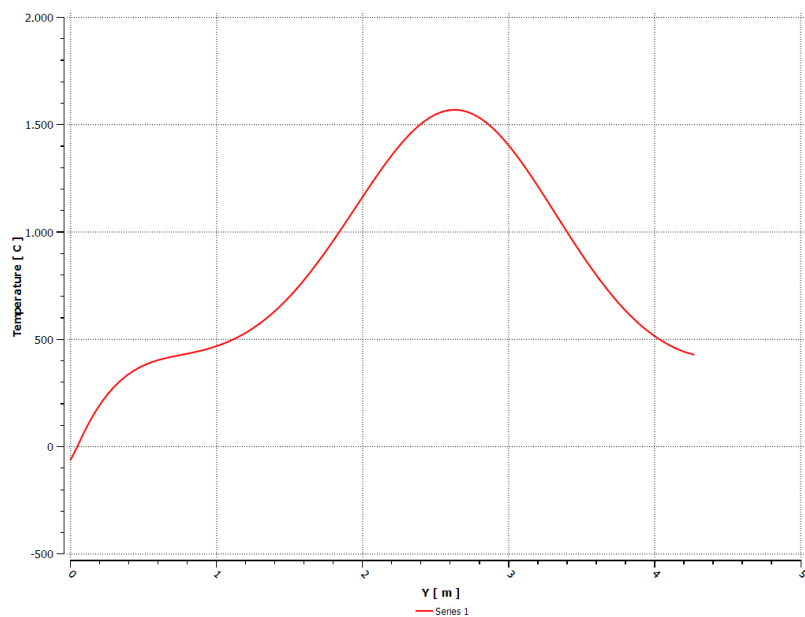


**Figure 8: Axial Temperature Distribution at the Fuel Center Line.**

According to the distribution shown in Figure 8 it was possible to determine the maximum temperature of the fuel which reaches a value of 1576°C, being much lower than its melting value which is around 3000°C, besides being below that obtained with the use of the conventional fuel with UO<sub>2</sub>, where Westinghouse itself reports a value of 1788°C. This lower value was expected since the coefficient of thermal conductivity of the MOX is higher than the thermal conductivity of UO<sub>2</sub>. The region of higher temperature is located just above the center of the bar, which is expected from a non-conservative analysis since even the shape of the temperature profile differs from an ideal analysis, which would have a cosine behavior.

In 2018, Martínez, using a similar methodology, obtained consistent values regarding the maximum fuel temperature as well as the maximum value reached by the cladding. The latter was also analyzed in the present work so that a radial temperature distribution was obtained to identify the maximum values reached in the other components of the fuel rod, as shown in Figure 9.

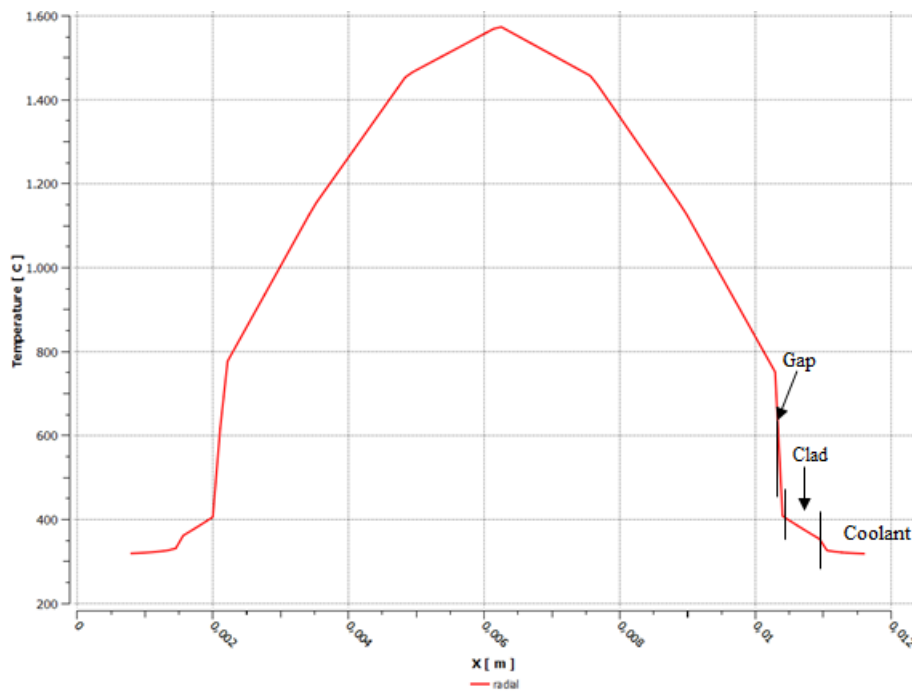


**Figure 9: Radial Distribution of the Temperature in the Hottest Bar in the Fuel Assembly.**

From Figure 9, it was possible to identify the maximum temperatures reached by other components of the fuel rod, among them the cladding, which for the present study presented a maximum value of approximately 400°C. Taking into account the data reported by the reactor manufacturer, this can be considered a good result, since the accepted limit for Zircaloy is 1204°C, thus avoiding possible oxidation and consequently its degradation.

According to the results presented, a comparison was made with the data reported by the Westinghouse construction company, in which it was verified that the design limits were not exceeded and that, in turn, were lower than the commonly found operating limits.

In addition, to verify that the data obtained are in agreement with the reactor manufacturer itself, another comparison was made, but this time in relation to the literature. Santos in 2016 [5] conducted a thermohydraulic study of the hottest channel at cycle start conditions for several reactors, one of them being the AP1000 so that in this analysis the use of two types of fuel was considered. The first study was about the AP1000 having UO<sub>2</sub> fuel, in the second case, this fuel was replaced by a mixture of mixed oxides of uranium and thorium MOX (U, Th)O<sub>2</sub>.

Since the study conducted by Santos in 2016 was not through the same methodology applied in this study, we cannot validate the results presented in this article with data from Santos (2016). However, a comparison with its results was made to show that the model proposed in the present study, although being more robust and having as its main difference in relation to the model of Santos (2016), considering the dependence of material properties on temperature, was able to provide satisfactory initial results.

By applying the methodology proposed in the present work, one of the results obtained was the axial distribution of mean refrigerant temperature, as shown in Figure 10a, it is possible to observe that water leaves the reactor vessel with a maximum average temperature of 326, 5 ° C. Figure 10b presents the same distribution obtained by Santos (2016), which shows that the maximum temperature at the outlet is 317 ° C.

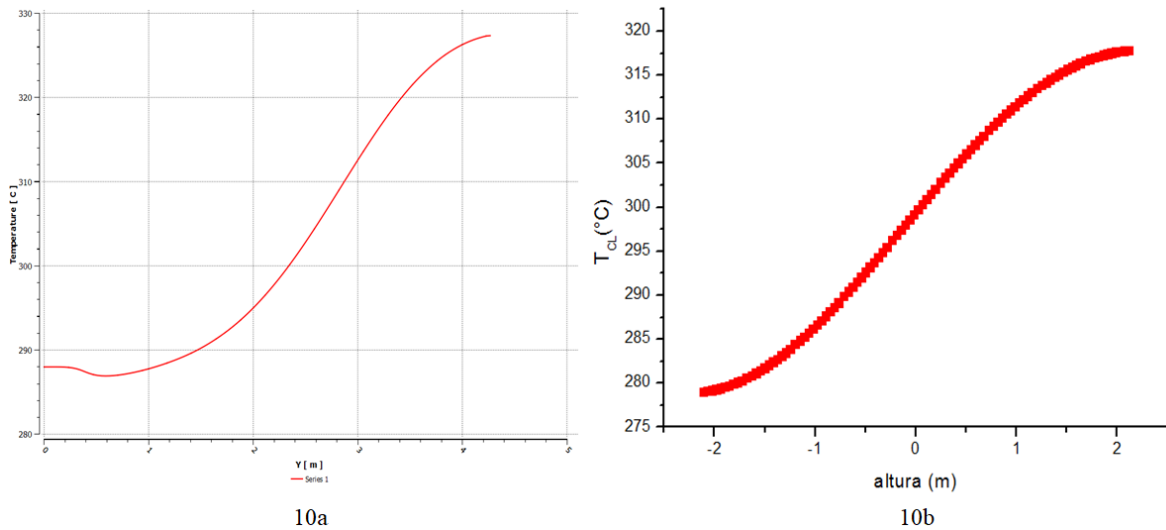


**Figure 10: Axial Distribution of Mean Coolant Temperature.**

The maximum temperature reached in the fuel is a parameter (like the others) that cannot be directly compared with the work of Santos (2016), however, it can be analyzed in order to be in the expected parameters for the process. In this study, it was considered 24% of  $UO_2$  in MOX and Santos (2016) used a percentage of 32% of  $UO_2$ , according to these percentages it is expected that the parameters reach higher values with the composition proposed by Santos (2016).

Evaluating the maximum temperature reached in the fuel, the present work had a maximum value of 1576 ° C and Santos (2016) 1615 ° C, however, this last value should be slightly higher because the parameters in such analysis should have been considered temperature dependent, however, most were admitted constant. The temperature dependence of the thermophysical properties of the fuel is illustrated in Figure 11.

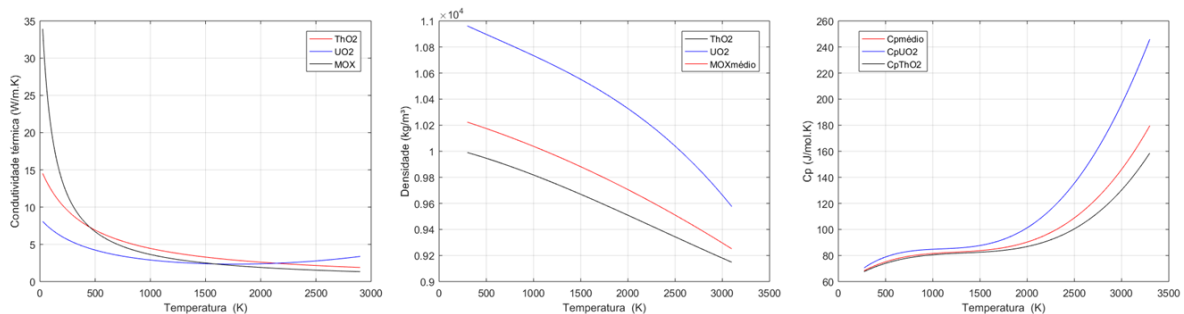


**Figure 11: Influence of Temperature on Thermophysical Properties.**

These corrections can be found in IAEA reports. According to Figure 11, it is possible to verify a significant variation of these properties with temperature, even in situations of normal reactor operation. Therefore, the result of Santos (2016) was expected to be slightly above that obtained in his study, if a more detailed analysis were performed.

The effect of this dependence can be confirmed by the study developed by Martínez in 2018 [14], which conducted a thermohydraulic study of the AP1000 reactor and evaluated the same design limits in case of constant and temperature-varying thermophysical properties. For the maximum temperature reached in the fuel, considering the constant properties, a value of approximately 1100 ° C was obtained, however, when it considered this dependence of the properties with the temperature, it obtained for the same maximum temperature, a value of approximately 1767 ° C. These results show that there is a direct and significant influence on the thermophysical properties of both the fuel and the refrigerant itself.

#### 4. CONCLUSIONS

A three-dimensional model was developed and implemented through the Computational Fluid Dynamics code to evaluate the thermohydraulic behavior of a typical fuel assembly of the AP1000 reactor using a mixture of uranium and thorium oxides (U, Th)O<sub>2</sub>.

The axial power distribution was obtained in the typical fuel assembly of the AP1000 reactor through a coupled neutronic-thermohydraulic calculation using the MCNP6 and Ansys CFX codes. From this distribution it was possible to notice that its maximum value tends to the center of the bar along with the iteration iterations, being a little above the same when reaching the convergence, in addition to an expected behavior compared to other publications in the literature.

The temperature profiles in the fuel assembly were determined, as well as the distribution of the coolant density and consequent the pressure drop. It was observed that the fuel reaches a maximum temperature of 1576°C being below the one reported by the reactor manufacturer, as well as the data published by Martínez in 2018, which, using a similar methodology, was able to perform a thermohydraulic analysis of the AP1000 reactor using conventional UO<sub>2</sub> fuel. The maximum temperature reached by the cladding was also evaluated and a value of approximately 400°C was obtained, showing a good result against the maximum reported by Westinghouse, which is 1204°C, eliminating a possible degradation of the material.

The present work studied a beginning of cycle (BOC) situation for a typical fuel assembly of the AP1000 reactor using a MOX of (U, Th)O<sub>2</sub>, making some simplifications in its original design to obtain a base methodology capable of representing numerically a situation to which the reactor was subjected. To the detriment of the development of a base methodology, a future refinement is sought taking into account other geometric elements, such as burnable poisons and spacer grids, in order to carry out studies of operational transients with loss of coolant.

From the comparisons made with the reactor builder (Westinghouse) and Santos's work in 2016, it is observed that with a more robust model, considering the dependence of the parameters with the temperature, obtaining the power density through a thermohydraulic

neutron coupling, wherein both cases the thermophysical properties were considered the temperature dependence, the results were within the acceptance range and could be improved.

## ACKNOWLEDGMENTS

First of all, I thank God for the peace of mind granted for the accomplishment of this work. A special thank-you should be made to my advisor Dr. Fernando Roberto de Andrade Lima for the confidence in my work and for having believed in my potential, from this, the opportunities granted. I am very grateful to Dr. Daniel Gonzáles Rodrigues for all the follow-up in the analysis process through the CFX code, as well as the accompaniment with Dr. Fernando Roberto de Andrade Lima in the construction of the academic's texts. I also like to thank Dr. Jesús Alberto Rosales García for his support regarding the neutronic analysis of nuclear reactors, as well as the knowledge acquired.

## REFERENCES

1. STEFANI G. L., Sobre a viabilidade de conversão de um reator avançado PWR com núcleo de  $UO_2$  para  $(U,Th)O_2$ , Doctoral thesis – UFABC, São Paulo, 275p (2016).
2. MAIORINO J. R., STEFANI G. L., MOREIRA J. M. L., ROSSI P. C. R.; SANTOS T. A., Feasibility to convert an advanced PWR from  $UO_2$  to a mixed U/ $ThO_2$  core – Part I: Parametric studies, *Annals of Nuclear Energy*, v. **102**, pp. 47-55 (2016).
3. MAIORINO J. R., STEFANI G. L., D'ÁURIA F. S., Utilization of thorium in PWR reactors – a first step toward a Th-U fuel cycles, *Proceedings of the 26<sup>th</sup> International Conference Nuclear Energy for new Europe*, Slovenia, September 11-14 (2017).
4. MAIORINO J. R., D'ÁURIA F. S., AKBARI-JEYHOUNI R., Na Overview of Thorium utilization in Nuclear Reactors and Fuel Cycles, *Proceedings of the 12<sup>th</sup> International Conference of the Croatian Nuclear Society, Zadar – Croatia, June 3-6 (2018)*.
5. SANTOS T. A., Desenvolvimento de um código mono canal para análise termo hidráulica de reatores PWR, Masters dissertation – UFABC, São Paulo, 96p (2016).
6. BASKARA R. F., WARIS., KURNIADI R., BASAR K., WIDAYANI, SAHIN S., Advanced Nuclear Reactor AP1000 with  $ThO_2-UO_2$  fuel, *Journal of Physics*, v. **1204**, conference series 012135 (2019).
7. SELIM H. K., AMIN E. H., ROUSHDY H. E., Using thorium based fuel in AP1000: Steady state analysis, *Arab Journal of Nuclear Sciences and Applications*, v. **51**, pp. 9-21 (2019).
8. IAEA, Thorium fuel utilization: Options and trends, <https://www-pub.iaea.org/books/iaeabooks/6395/Thorium-Fuel-Utilization-Options-and-Trends> (2002).
9. WNA, Thorium, <http://world-nuclear.org/information-library/current-and-future-generation/thorium.aspx> (2017).
10. WNA, Advanced Nuclear Power Reactors, <http://www.world-nuclear.org/information-library/nuclear-fuel-cycle/nuclear-power-reactors/advanced-nuclear-power-reactors.aspx> (2018).
11. MAIORINO J. R., SANTOS A., PEREIRA S. A., The utilization of accelerators in subcritical systems for energy – R&D program, *Brazilian Journal of Physics*, v. **33**, pp.267-272 (2003).

12. WESTINGHOUSE ELETRIC COMPANY, AP1000 Pressurized Water Reactor, <http://www.westinghousenuclear.com/New-Plants/AP1000-PWR> (2016).
13. BUSSE A. L., MOREIRA J. M. L., MAIORINO J. R., Rejeitos radioativos em reatores PWR quando do descomissionamento, *Proceedings of the 9th Congresso brasileiro de Planejamento Energético*, Florianópolis, August 25-27 (2014).
14. MARTÍNEZ L. A., Simulación termohidráulica de um conjunto combustible del reactor nuclear AP1000, Bachelor thesis – INSTEC, Havana, 83p (2018).